IMPACT OF COOLING INJECTIOIN ON THE TRANSONIC OVER-TIP LEAKAGE FLOW AND SQUEALER AEROTHERMNAL DESIGN OPTIMIZATION

Z. Wang
University of Michigan-Shanghai Jiao Tong University Joint Institute, **Shanghai, China**
wangzhaoguang1991@hotmail.com

Q. Zhang[1,2]
[1]University of Michigan-Shanghai Jiao Tong University Joint Institute, **Shanghai, China**
[2]School of Engineering and Mathematical Sciences
City University London, United Kingdom EC1V 0HB
Corresponding Author, Email: Qiang.Zhang@city.ac.uk

Y. Liu
University of Michigan-Shanghai Jiao Tong University Joint Institute
Shanghai, China
yliume@umich.edu

L. He
Department of Engineering Science
University of Oxford
Oxford, UK
Li.He@eng.ox.ac.uk

ABSTRACT

In the present work, the effect of coolant injection on the Over-Tip-Leakage (OTL) flow and squealer designs has been investigated in a transonic flow regime. After an experimental verification of the computational tool adopted for capturing transonic flow characteristics, a series of quasi-3D computational analyses were carried out to reveal and understand the cooling jet - OTL flow interaction at various hole locations and inclination angles. The results indicate that the performance rankings between flat tip and squealer tip designs might be altered by the addition of cooling injection. Full 3D conjugate heat transfer analyses demonstrate that partially replacing the squealer cavity with a simple flat shaped configuration in the rear transonic flow portion would offer a much improved coolablility without paying extra aerodynamic penalty.

INTRODUCTION

Modern turbine blade tip has to be effectively cooled to survive the extremely high heat load in the engine operating condition, even though most typical tip design concepts were initiated by the aerodynamicist to control the Over-Tip-Leakage (OTL) loss. The cooling injection within the narrow tip gap clearance would add much more complexity to the OTL flow structure, thus greatly vary tip heat load distribution. In practice, the tip aerodynamic design and the cooling design have to be an iterative process.

The mixing process between OTL flow and the coolant and related heat transfer are different from most of the other film cooling in the gas turbine. Generally the injected coolant either impinges onto the adjacent casing wall, or has to interact with highly three-dimensional vortical flow structures associated with winglet or squealer tip designs. As addressed by Bunker [1], the primary intention for an efficient tip film cooling is to reduce heat flux with minimal coolant amounts (not to block the leakage flow from entering the tip gap, though this effect may be present to a small degree). There have been many studies which focused on the heat transfer and film cooling effectiveness of tip injection. Kim et al. [2] presented an early review on the effects of coolant injection on heat transfer. They reported that, for a given tip geometry, the cooling effectiveness was highly dependent on the coolant hole shape and injection location. The performance of different cooling hole shapes and geometries has been studied by Kim and Kim [3] and Lee and Kim [4]. According to Newton et al. [5], coolant holes placed at the separation bubble have a better performance than at the reattachment zone in reducing the tip heat load. Their flow visualization and pressure data revealed that injecting coolant can significantly alter the fluid dynamics of the OTL flow. This observation is also consistent with the experimental study by Yoon and Martinez-Botas [6]. The understanding in common is that, the interaction between the separation bubble and the narrow tip passage prevents the coolant expanding into the freestream, forces the coolant into a closer contact with the tip surface, and thus leads to a better film cooling performance. Ahn et al. [7] compared the cooling performance of plane and squealer tips with cooling holes located along the camber line or along the pressure side. Pressure-side cooling injection was identified as a better choice. For a squealer tip design, Hofer and Arts [8] found out that increasing the coolant mass flow rate increases the resistance to the OTL flow and the tip heat transfer is reduced accordingly. Similarly for a winglet tip studied by Zhou et al. [9], the average cooling effectiveness increases and the heat load reduces with more coolant mass flow ratio. Narzary et al. [10] and Li et al. [11] investigated the effect of coolant density ratio on cooling effectiveness, and concluded that the heavier density coolant could adhere to the surface and result in a higher film cooling effectiveness. The relationship between the blowing ratio and cooling effectiveness has also been studied by Lu et

al., [12], Ahn et al. [7], Mhetras et al. [13] and Kwak and Han [14], etc.

Researchers have also paid some attentions on the effect of tip cooling injection on the OTL flow structure and aerodynamic loss. An early study of OTL flow by Chen et al. [15] indicated that, introducing an appropriate secondary jet into the tip gap for both flat and squealer tips has a tendency to reduce the discharge coefficient of the tip leakage, with a more or less fixed total mass flow rate at the tip gap exit under both subsonic and transonic conditions. Hohlfeld et al. [16] and Couch et al. [17] investigated the effect of blowing coolant from the dirt purge holes, and reported that the reduction of OTL flow by the secondary jet is significant for the small tip gap (less beneficial for the large tip gap). For a low-speed squealer tip, Krishnabanu et al. [18] showed that the cooling injection could partially block the gap region by reducing the area available for the mainstream flow leaking through the tip gap. It has also been recognized that, the blockage effect can be further optimized by the right location (i.e., separation vortex region, Niu and Zang [19]) and right injection orientation (i.e., against the leakage flow, Lim et al. [20] and Curtis et al. [21], Hamik and Willinger [22]).

Due to the complex interactions between the coolant and the OTL flow at different tip designs, there are some discrepancies among the open literature in terms of the ratings of aerodynamic loss associated with tip cooling injection. For a winglet tip, Zhou et al. [9] reported a 6% reduction in aerodynamic loss with the introduction of an engine representative coolant mass flow rate in their low speed experiments. However, with the same geometry in a transonic experimental condition, O'Dowd et al. [23] observed a decrease in aerodynamic loss with cooling injection. A comparison of leakage loss for a cooled flat tip and a cooled squealer tip under a low speed (subsonic) condition was made by Zhou and Hodson [24]. Their results showed that cooling injection in small amounts decreased the leakage flow for the flat tip, but an opposite trend was identified for the squealer tip. Hofer and Arts [8] found that the effect of cooling on the overall mass-weighted loss coefficient is marginal for the two squealer geometries investigated in their transonic experimental study. Wheeler and Saleh [25] studied the effect of adding cooling slot to flat and squealer tips in transonic OTL flow condition. Their results consistently show that there is a potential to reduce tip leakage losses by tip cooling.

The transonic nature of OTL flow for some HPT blade tip designs has only been recognized in recent years (Wheeler et al. [26], Zhang et. al. [27], Zhang and He [28]). There are still limited published data regarding cooled tip in transonic conditions. The choking behavior and shock mechanism in the transonic OTL flow are special features which we should consider during the iterative aero-cool-aero design loop for blade tip of HP turbines.

The present numerical study is aimed firstly to gain some further understanding related to the transonic OTL flow structure with cooling injection for a flat tip and a squealer geometry through a series of quasi-3D analyses. Effects of cooling hole location and orientation are studied. Based on these analyses, a new cooled partial frontal squealer design is proposed and numerically tested with a full 3D conjugate analysis. The aero-thermal performance are demonstrated and ranked against a typical full squealer tip design.

NOMENCLATURE

d	cooling hole diameter
g	height of tip gap
h	depth of squealer cavity
HPT	High Pressure Turbine
l	distance along gap exit at suction side
m''	mass flux
$\dot{m}$	mass flow rate
n	refractive index
OTL	Over-Tip Leakage
p	pitch of quasi-3D domain (hole spacing)
P	pressure
PS	pressure side
RANS	Reynolds-Averaged Navier-Stokes
s	total length of gap exit at suction side
SS	suction side
T	temperature
ΔT	temperature difference of coolant and mainstream
w	width of squealer rim
y	pitch-wise direction of quasi-3D domain
z	span-wise distance from tip surface
α	cooling hole angle
ζ	loss coefficient
ρ	density
∇^2	Laplacian

Subscripts

0	total
c	coolant
CHT	Conjugate Heat Transfer
in	mainstream inlet
MID	middle section
out	mainstream outlet
PS	near pressure side
s	static
SS	near suction side
w	blade surface

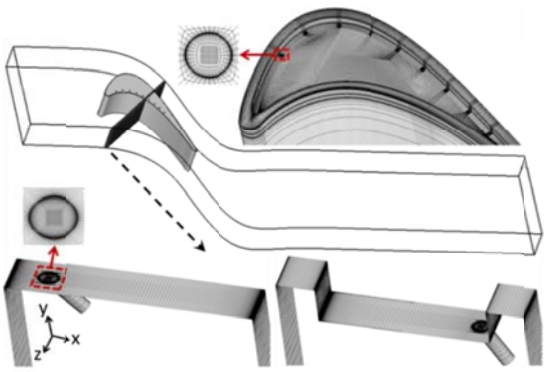

Fig. 1 Computational domain and meshes.

COMPUTATIONAL METHOD

A commercial CFD solver, ANSYS FLUENT 14.5, was employed in the present numerical study. This software solves the three-dimensional, steady, turbulent form of the Reynolds-Averaged Navier-Stokes (RANS) equations with a finite volume method. Two turbulence models, K-Omega SST and Spalart-Allmaras model were initially chosen for solving some typical cases in the present study. Negligible differences were identified from the resulting global performance parameters and detailed local flow structure. Spalart-Allmaras turbulence model was employed for solving all the cases in the present study. (It has been reported by Wheeler et al. [26] that the accuracy of CFD predictions for high speed tip flow is less dependent on the choice of turbulence model than for low speed.)

Figure 1 presents the three-dimensional computational domain and meshes employed in the present study. The computational domain consists of one single HPT blade with periodic boundary conditions. The same blade profile was employed by Li et al. [29].

The conventional boundary conditions for turbomachinery flow calculations were used. The stagnation pressure $P_{0,in}$, stagnation temperature $T_{0,in}$, and flow angle are specified at the inlet (one axial chord length upstream of the leading edge), and the static pressure $P_{s,out}$ is specified at the exit of the computational domain (four axial chord length downstream of the trailing edge). A typical transonic flow condition is established: the inlet-exit pressure ratio $P_{0,in}/P_{s,out}$ is 2, the exit Mach number is 1.03, and the exit Reynolds number based on axial chord is 1.54×10^6. For the cases with cooling injection, the coolant total pressure ratio $P_{0,c}/P_{0,in}$ is maintained as 1.1, which is close to a typical engine cooling design condition in practice. The inlet total temperature $T_{0,in}$ is set as *450K*. Symmetric boundary condition was imposed at the end of the domain (blade and flow region) opposite the tip.

Full 3-D conjugate calculations were conducted for two different tip designs with cooling injection (full squealer tip and partial frontal squealer described later). To study the detailed flow structure of cooling injection with affordable computational cost in the parametric study (also to better resolve the flow near the cooling hole), a quasi-3D domain is extracted along the streamline direction from the transonic region in the full 3D computational domain (a geometrical subset of a full blade passage), as shown in Fig. 1.

A commercial software, Pointwise, was employed to generate structured meshes for both 3D and quasi-3D domains (with and without cooling injection). In the grid-independence study performed, special attention was paid on the grids density (near-wall grid size/expansion ratio) for the cooling hole region and near tip surface. Figure 2 shows local OTL mass flux distribution obtained with three density levels of grids at a location near the exit of the tip region. The maximum local difference between all three grids is less than 2%. The differences in the averaged OTL mass flow rate are negligible. 1.48 million and 5.76 million grids were used for the quasi-3D and full 3D calculations, respectively.

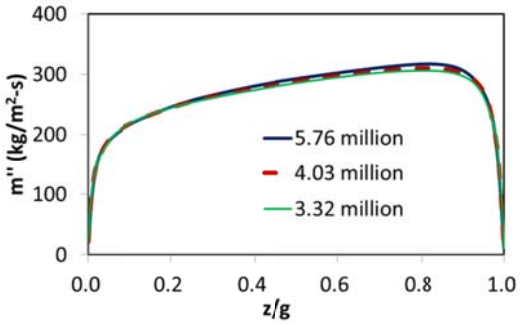

Fig. 2 Grid independence study: local OTL mass flux distribution at the exit of the tip region, obtained with three density levels of grids.

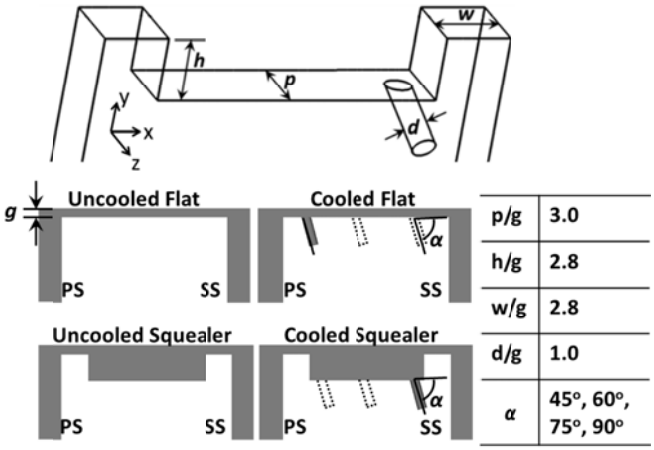

Fig. 3 Schematics of cooled/uncooled flat and squealer tip geometries investigated in the quasi-3D calculations.

For all cases investigated in the present study, the tip clearance height (g) is equivalent to 1% of the blade span (a typical engine design value). Figure 3 presents schematics of cooled/uncooled flat and squealer tip geometries investigated in the quasi-3D calculations.

To isolate the aerodynamic impact of cooling injection, same total temperature was applied to the mainstream inlet and the cooling injection for all the quasi-3D cases. Adiabatic wall boundary conditions were imposed on all the tip surfaces.

EXPERIMENTAL VALIDATION

To validate the results of quasi-3D simulations, a shadowgraph system (Fig. 4) was set up to capture the separation bubble and the shock wave within the tip gap, where strong density variation was expected. Two convex lenses with focus length 15cm and a grating converted the light emitted from a projector into parallel light, which passed across the tip

gap. A CCD camera was arranged to capture the shadowgraph image.

The tip gap height and length in the experiment were scaled up to five times of the one in the CFD simulation for higher-resolution shadowgraph image. (The change of Reynolds numbers has been considered in CFD simulations.) The width of the passage is ten times of the gap height to avoid side wall effect. Same inlet and outlet pressures were applied in both CFD and experiments. The fluctuation of the inlet total pressure in the experiment was within ±0.5%.

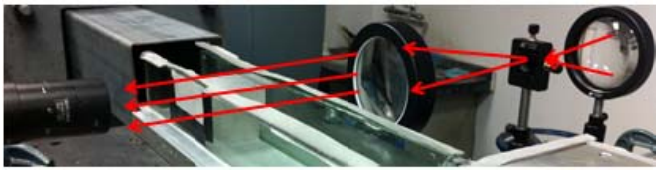

Fig. 4 Shadowgraph system employed for CFD validation.

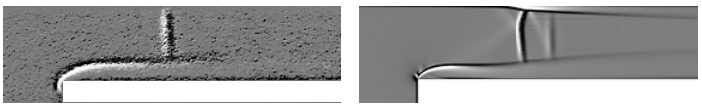

(a) (b)

Fig. 5 (a) shadowgraph image from experiment, (b) $\nabla^2\rho$ contour from CFD.

As stated by F. J. Weinberg [30], the light intensity of a shadowgraph is proportional to the Laplacian ∇^2 of the refractive index n of the medium. Moreover, according to the Gladstone-Dale relation [31], for gases the density ρ is proportional to n-1, where n is the refractive index. Hence the light intensity shown in a shadowgraph is proportional to $\nabla^2\rho$.

Figure 5 compares the shadowgraph obtained from experiment to the $\nabla^2\rho$ contour by CFD. Both results share the same shock wave location and similar shape of the separation bubble. The second reflected shock wave shown in the CFD result was not observed in the experiment due to relatively weak density variation.

RESULTS AND DISCUSSIONS

Cooling jet - transonic OTL flow interactions

Figure 6a presents the Mach number distributions along the middle of the quasi-3D computational domain for uncooled and cooled flat tip cases with cooling hole placed at three tip locations. The inclination angle is set as 45°, which is an optimized angle, as discussed later in Figure 10. These 2D contours indicate that the OTL flow for all cases is transonic. For the uncooled case, the flow is choked near the pressure side separation bubble. With the addition of cooling injection, the choking region is moved close to the exit corner of the cooling hole. The existence of cooling jet core is illustrated by an iso-volume of fluid stagnation pressure ($P_{0,c}/P_{0,in}$ >1.01), as shown in Fig. 6b. This iso-volume and all streamlines nearby are colored by Mach number. Figure 6b illustrates that the coolant with higher stagnation pressure ejects from an opposite 45° angle, bends in the direction of the OTL flow, and impinges onto the adjacent casing wall. For the case with coolant hole placed near the pressure side location, a large separation zone is confined in front of the cooling jet.

Figure 7 presents Mach number contours with secondary flow vectors along two cut-planes downstream of the cooling hole. Most of the OTL flow is in choking condition near the edge of the cooling hole exit. Two kidney-shaped low subsonic regions are evident in the same contour plane. The cooling jet forms a pair of counter-rotating vortices as it travels along the gap after its initial bending.

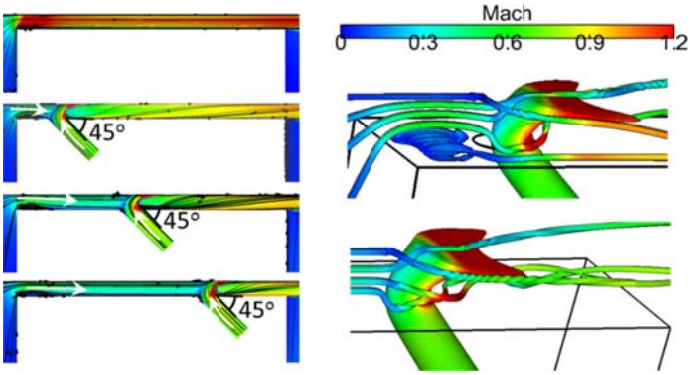

(a) (b)

Fig. 6 Flow structures of uncooled and cooled flat tips including (a) Mach number distributions along the domain mid-plane, and (b) cooling jet core and streamlines colored by Mach number.

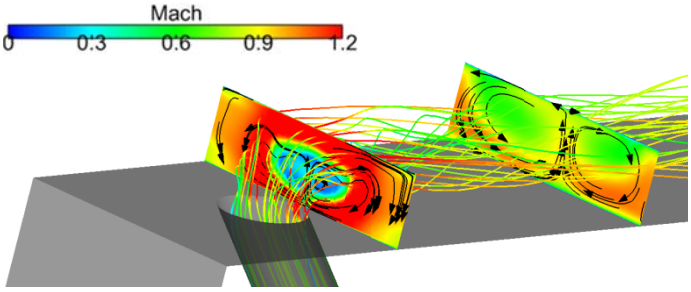

Fig. 7 Mach number contours with secondary flow vectors along two cut-planes downstream of the cooling injection.

Figure 8a illustrates the Mach number distributions along the domain mid-plane for squealer tips with cooling holes placed at various cavity locations. The inclination angle 60° was chosen based on the optimization result shown in Figure 10. A large recirculating vortex is formed in the squealer cavity for the uncooled case. With cooling injection, this large vortex breaks into smaller ones. The leakage flow is still transonic, with the choking throat located above the suction side rim. Figure 8b shows that the cooling jet core loses its initial momentum due to the strong mixing with the cavity flow, and the impingement to the casing wall is much weaker compared with the cooled flat tip case.

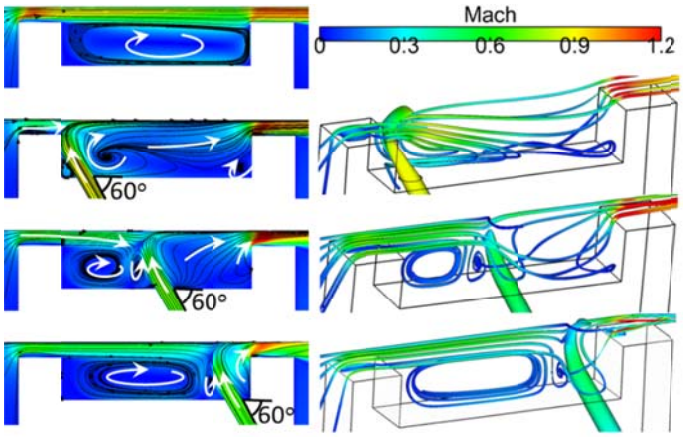

(a) (b)

Fig. 8 Flow structures of uncooled and cooled squealer tips including (a) Mach number distributions along the domain mid-plane for uncooled and cooled squealer tips, and (b) cooling jet core and streamlines colored by Mach number.

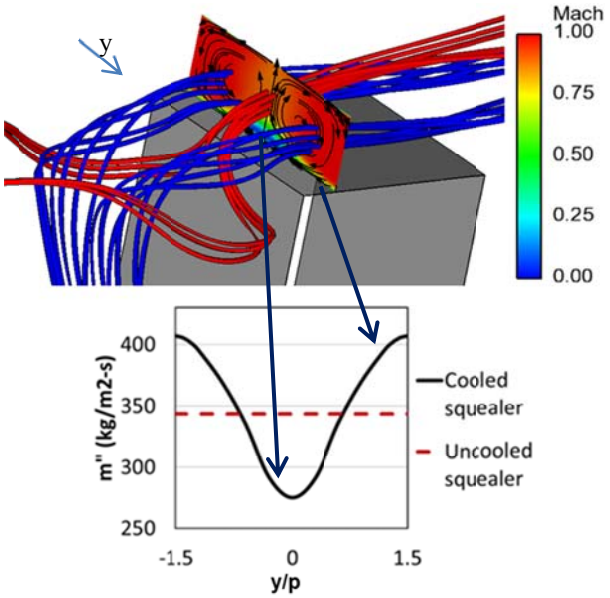

Fig. 9 Interactions between cooling injection and the squealer OTL flow, illustrated by a Mach number contour, streamlines from the cooling jet (blue) and incoming OTL flow (red), and span-wise averaged mass flux distributions.

Figure 9 further illustrates the interactions between cooling injection and the squealer OTL flow. For the case with cooling jet located near the suction side rim and $\alpha = 60^o$, a cut-plane colored with Mach number is made above the suction side rim (near inner edge). For most of the region in this plane, the flow is in a choking condition. The coolant ejecting from the cavity floor forms a pair of counter-rotating vortices when it passes over the rim region, as indicated by the secondary flow vectors shown in Fig. 9. Due to the blockage of coolant jet, there is a substantial low subsonic region behind the core of the cooling jet. On the other hand, the counter-rotating vortical flow could drag the near wall low momentum fluids away, and bring more adjacent fluids down to the squealer rim. The separation bubble normally occurring over an uncooled squealer rim cannot be clearly identified due to the impact of this strong secondary flow. The corresponding span-wise averaged mass flux distribution along this cut plane is also shown in Fig. 9. Compared with an uncooled squealer case (red dashed line), the local reduction of leakage flow behind the cooling injection (blockage effect) is counteracted by the removal of separation bubble under the vortex pair. Such mechanism does not exist for the cooled flat tip cases investigated in the present study.

Rankings between a cooled flat and cooled squealer

Figure 10 summarizes the overall OTL mass flow rate at the exit of the tip gap for all the quasi-3D cases investigated. All mass flow rate values are normalized with the result from an uncooled flat tip. Without cooling injection, a squealer tip brings a 10% reduction in OTL mass flow rate compared with the flat tip design in the present transonic condition. For all the cooled flat tip cases (solid lines), the exit mass flow rate is much less than the uncooled case due to the blockage effect and local reduction of effective choking area, as demonstrated earlier in Fig. 6. The mass flow is further reduced with smaller inclination angle, and closer location to the pressure side. An optimal 13.2% reduction of OTL mass flow rate can be achieved when the cooling hole is placed near the pressure side edge with $\alpha = 45^o$.

In contrast, cooling injection brings an opposite trend to the squealer tip: all cooled squealer has a slightly higher OTL flow rate than the uncooled one. The dependence of the OTL mass flow rate on the cooling hole location and inclination angle is relatively weak. Slightly better performance can be observed for the case with $\alpha = 60^o$, near the suction side rim. At a 45^o inclination angle, all cooled squealer designs result in a higher OTL mass flow than the cooled flat tip, no matter where the cooling hole is located. Such behavior is due to a weakened cooling jet blockage effect and the induced counter-rotating vortices above the suction side rim which can reduce (or partially remove) the separation bubble in the choking throat region (as illustrated in Fig. 9) .

For all the quasi-3D calculations, the coolant inlet total pressure is maintained constant ($P_{0,c}/P_{0,in}$ = 1.1). The coolant mass flow would be different for different tip geometries due to the variation of local pressures. Figure 11 shows the break-up details of overall OTL exit flow rate, incoming flow rate from the pressure side, and the coolant mass flow rate, for a cooled flat tip (α =45^o, near PS corner) and a cooled squealer tip (α = 60^o, near suction side rim). The coolant mass flow rate for the squealer case is slightly less than the coolant consumed by the flat tip case (0.26 *vs* 0.28). An additional calculation for a cooled flat tip was also conducted by setting a same coolant inlet mass flow (0.26) and the result indicates that the overall OTL mass flow rate for squealer is consistently higher than the flat case. A rather simple message can be obtained by comparing these numbers shown in Fig. 11: a cooled flat tip

outperforms a cooled squealer in terms of OTL mass flow in the transonic flow condition (with either the same pressure ratio or the same amount of coolant mass flow). Such observation partially agree with the results by Zhou and Hodson [24] (in low speed) and Wheeler and Saleh [25] (cooling slot).

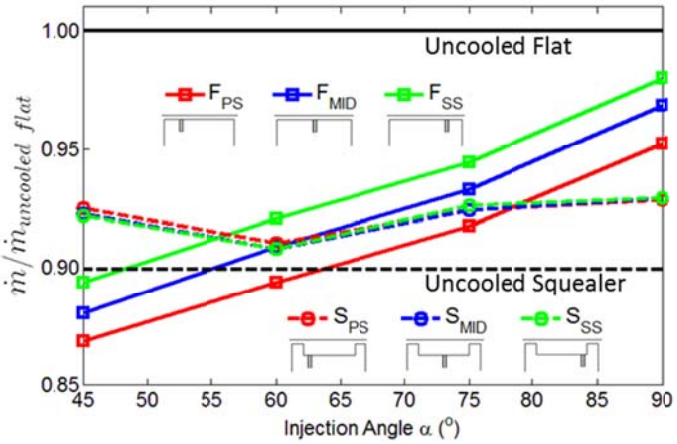

Fig. 10 Overall OTL mass flow rate at the exit of the tip gap for all the quasi-3D cases investigated.

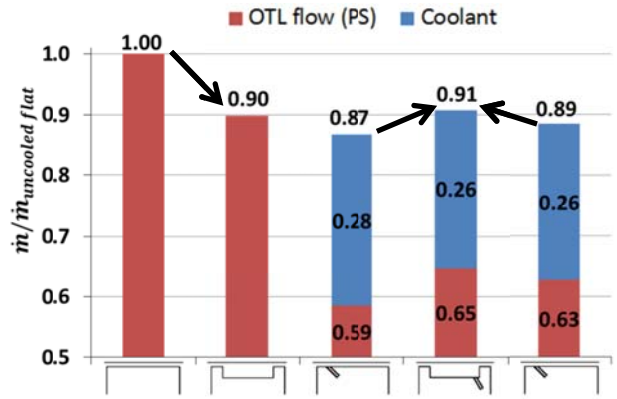

Fig. 11 Break-up details of mass flow rate for a cooled flat tip (α =45°, near PS corner) and a cooled squealer tip (α = 60°, near suction side rim).

Note that the current ratings between cooled flat and squealer tip geometry are only based on results obtained in transonic flow regime with one typical hole spacing (p=3g). Effect of the temperature ratio between the coolant and the OTL flow has not been considered. Also in practice, the squealer cavity flow is highly three-dimensional with different strengths of cavity vortices. These quasi-3D analyses can only provide a qualitative trend and serve as a general guide for further 3D design optimization.

Partial frontal squealer concept

In the real engine operating condition, the rear region of a squealer tip often gets burned out by the local high heat load, especially near the suction side rim. It is also difficult to place cooling holes in this region due to the limited space available.

The flow over the frontal tip region is subsonic, and the advantage of squealer over flat tip design in low speed regime has been validated and widely accepted. However, based on the understandings from the previous quasi-3D analyses, in the transonic regime, we cannot get the expected aerodynamic benefit from the squealer compared with the flat design once both get cooled. Instead of planning complex cooling schemes around the squealer geometry, maybe it is not a bad idea to completely discard the squealer design while the local OTL flow becomes transonic.

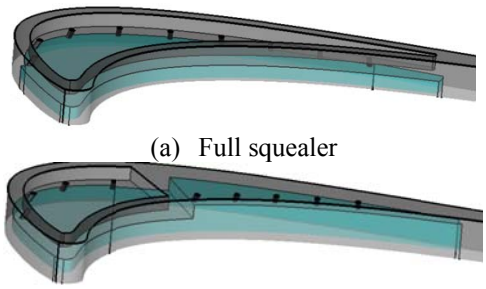

(a) Full squealer

(b) Partial frontal squealer

Fig. 12 Two cooled squealer investigated in the present study (internal wall colored in blue).

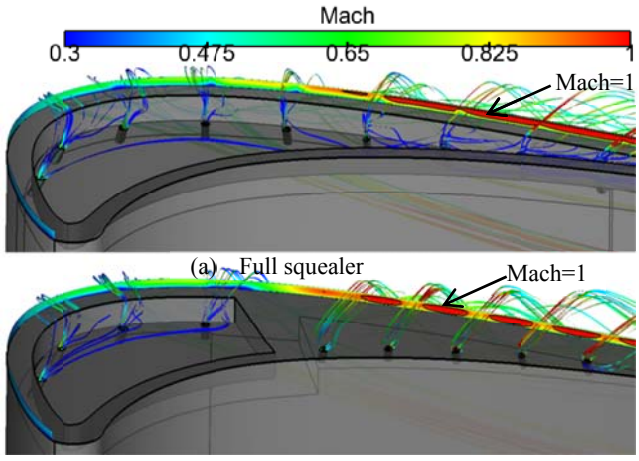

(a) Full squealer

(b) Partial frontal squealer

Fig. 13 Mach number contour distribution along the tip gap exit for two tip cooling designs.

In this case study, a partial frontal squealer design is proposed and compared with a conventional full squealer with full 3D conjugate analyses. The two tip cooling geometries are shown in Fig. 12. Nine cooling holes are evenly placed over the tip region. The internal wall thickness was set to be two times of the tip gap height (2g). The heat transfer coefficient for the internal wall was assumed to be a uniform value of 1000 w/m^{2}k. A temperature ratio ($T_{0,c}/T_{0,in}$) *of 0.5* is specified for the coolant inlet. The same coolant temperature applies to all the internal wall boundaries as the fluid driving temperature. The

coolant total pressure ratio is kept as $P_{0,c}/P_{0,in}$ = 1.1. These parameters are largely in the same scale as the typical engine design. The material properties of the blade are set to be same as ASTM 310. The thermal conductivity is assigned to be a polynomial function of temperature.

Figure 13 presents Mach number contours along the tip gap exit (above the suction side edge) for the two cooled squealer cases. The flow is subsonic in the frontal region. Very similar patterns can be observed for both cases. The conventional wisdom about squealer tip should work well in this subsonic flow regime, as reported by many early studies. In the rear part of the tip region, most of the exit OTL flow is choked (the dark lines indicate Mach=1, as shown in Fig. 13). Discrete cooling injections locally disturb the OTL flow and reduce the choking area. Larger choking region can be identified for the full squealer case, as shown in Fig. 13.

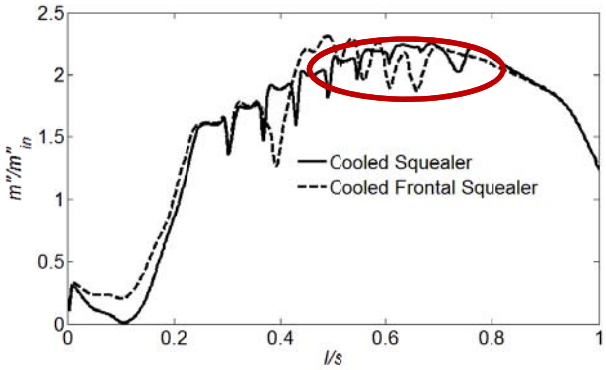

Fig. 14 Span-wise averaged mass flux distribution of the OTL flow along the gap exit (along suction surface side)

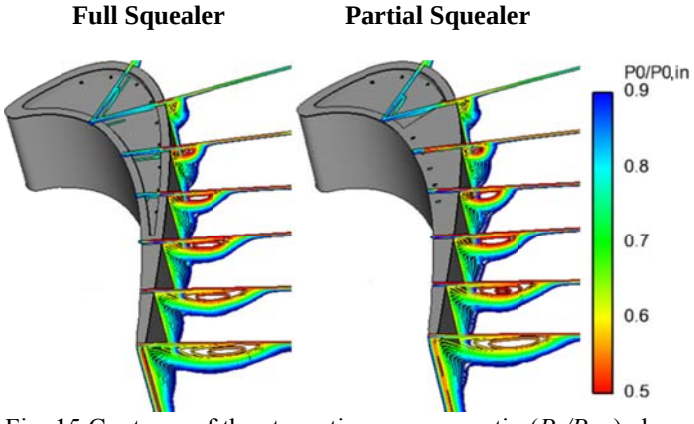

Fig. 15 Contours of the stagnation pressure ratio ($P_0/P_{0,in}$) along the passage.

Figure 14 shows span-wise averaged mass flux distributions of the OTL flow along the suction side exit edge. The general trend between the two cooled squealers is very similar. The partial frontal squealer gives a higher local leakage flow near the leading edge region (l/s < 0.2). This is due to a weakened recirculating cavity flow due to a reduced cavity size. It is expected that the performance in this region could be improved by further optimization of the cavity depth and cooling hole location. For the region of l/s > 0.5 (circled in red), the cooling injections cause more reductions to the leakage flow for the partial frontal squealer, which has a simple flat shape in this region.

Figure 15 presents stagnation pressure ratio contours ($P_0/P_{0,i}$) along the passage. Negligible differences could be identified for these two cooled squealer cases, i.e., replacing the rear squealer cavity does not introduce apparent extra aerodynamic penalty.

Table 1 summarizes the overall OTL mass flow rate and loss coefficient for both cooled squealer cases. The overall loss in kinetic energy was evaluated based on the equation listed below (similar forms previously used by [32, 8, 23]).

$$\zeta = 1 - \frac{(\dot{m}_c Cp_c T_{0,c} + \dot{m}_m Cp_m \cdot T_{0,m})\left(1 - \left(\frac{P_{exit}}{P_{0,exit}}\right)^{\frac{\gamma-1}{\gamma}}\right)}{\dot{m}_m Cp_m \cdot T_{0,m} \cdot \left(1 - \left(\frac{P_{midspan}}{P_{0,m}}\right)^{\frac{\gamma-1}{\gamma}}\right) + \dot{m}_c \cdot Cp_c \cdot T_{0,c} \cdot \left(1 - \left(\frac{P_{midspan}}{P_{0,c}}\right)^{\frac{\gamma-1}{\gamma}}\right)}$$

Note that this loss coefficient is a global thermodynamic definition, which includes contributions due to viscous effects and heat transfer between the mainstream, cooling flow, and the blade wall in the present conjugate analysis. The differences of all the global values between two squealer designs are negligible, as shown in Table 1, where $\dot{m}_{OTL}$ represents the total OTL mass flow rate.

In the present study, no further attempt was made to optimize the partial frontal squealer geometry for a better aerodynamic performance. Potentially a reduction of OTL mass flow and loss is possible based on the previous quasi-3D analyses.

Table 1 summary of OTL mass flow and loss coefficient

	Full squealer	Partial frontal squealer
$\dot{m}_c$ (kg/s)	0.0034	0.0033
$\dot{m}_{OTL}$ (kg/s)	0.0376	0.0379
ζ	0.130	0.130

Figure 16 presents surface temperature ratio ($T_w/T_{0,in}$) distributions for the two cooled squealer cases. Quantitative comparisons are also made by comparing the temperature ratios along a cut plane in the rear region of the tip surface. For the full squealer case, the heat load is very high near the squealer rim ($T_w/T_{0,in}$ >0.8). Clearly, more cooling supply is required to further lower the surface temperature. In contrast, replacing the squealer cavity with a flat shape offers a uniformly lower surface temperature ($T_w/T_{0,in}$ <0.75). This is due to a good coverage of the coolant over the tip surface, and more importantly, an effective heat conduction through internal cooling.

All these conjugate analyses in the present study support a key message: partially replacing the squealer cavity with a flat shape in the transonic flow regime would offer a much improved coolablility without paying extra aerodynamic penalty.

In practice, squealer tip design also serves the purpose of minimizing mechanical damage in the event of a rotor-shroud rubbing. Therefore, the partial flat tip region should be carefully determined to balance both the coolability and the mechanical durability in the detailed design process.

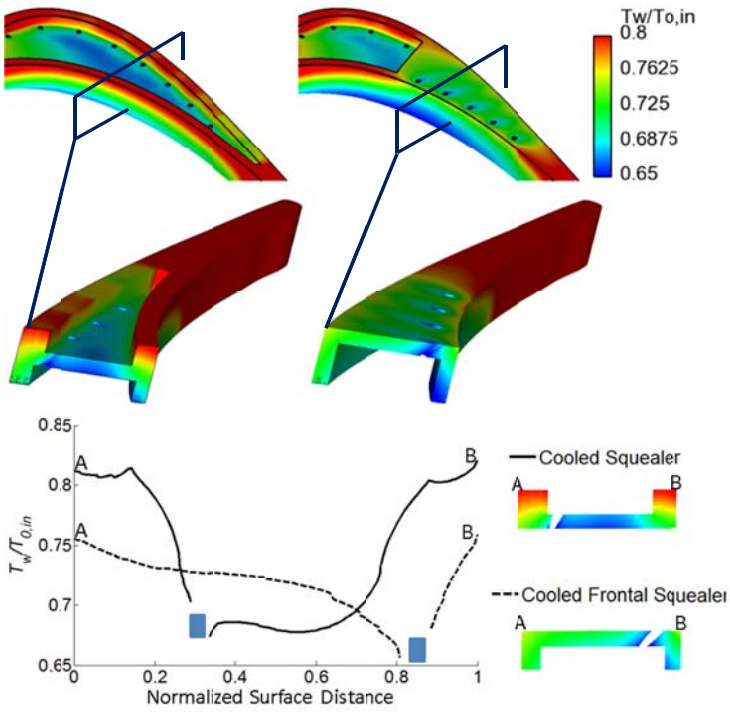

Fig. 16 Comparisons of surface temperature ratio ($T_w/T_{0,i}$) for two cooled squealer cases.

SUMMARY AND CONCLUSIONS

The effects of cooling injection on the OTL flow and squealer design in a transonic flow regime are numerically investigated in the present work. A series of quasi-3D analyses were carried out by using a CFD solver verified for transonic tip flows, to illustrate and understand the cooling jet - OTL flow interactions at various hole locations and inclination angles.

The present results indicate that the rankings of predicted performances for different tip design could be altered by the addition of cooling injection: a cooled flat tip can outperform a cooled squealer in terms of OTL mass flow under the transonic flow condition. For a cooled squealer, the cooling jet blockage effect is relatively weak, a pair of counter-rotating vortices are induced above the suction side rim, which can partially remove the separation bubble in the choked throat region, hence reducing the effectiveness of the squealer for the transonic part of the tip.

The results of a full 3D conjugate analysis demonstrate that partially replacing the squealer cavity with a flat shaped configuration in the rear transonic flow region may potentially offer a much improved coolablility without paying extra aerodynamic penalty.

For practical designs, the geometries of the frontal squealer and cooling hole locations could be further optimized for improved aerodynamic and thermal performance.

ACKNOWLEDGMENTS

The authors gratefully acknowledge the support of Chinese National Science Foundation (51076102) and Shanghai Pujiang program (12PJ1405500) for funding this work.

REFERENCES

[1] Bunker, R. S., 2006, "Axial Turbine Blade Tips: Function, Design, and Durability," AIAA Journal of Propulsion and Power, Vol. 22, No. 2, 2006, pp. 271 – 285.

[2] Kim, Y. W., Downs, J. P., Soechting, F. O., Abdel-Messeh, W., Steuber, G., and Tanrikut, S., 1995, "A Summary of the Cooled Turbine Blade Tip Heat Transfer and Film Effectiveness Investigations Performed by Dr. D. E. Metzger," ASME J. Turbomach., 117(1), 1-11.

[3] Kim, Y. J., and Kim, S. M., 2004, "Influence of shaped injection holes on turbine blade leading edge film cooling," International Journal of Heat and Mass Transfer, 47:245–256.

[4] Lee, K. D., and Kim, K. Y., 2010, "Shape Optimization of a Laidback Fan-Shaped Film-Cooling Hole to Enhance Cooling Performance," International Journal of Heat and Mass Transfer, Vol. 53, pp. 2996–3005.

[5] Newton, P. J., Lock, G. D., Krishnababu, S. K., Hodson, H. P., Dawes, W.N., Hannis, J., and Whitney, C., 2007, "Aero-thermal investigation of tip leakage flow in axial flow turbines Part III- film cooling," ASME J. Turbomach., 131, p 011008.

[6] Yoon, J. H., and Martinez-Botas, R. F., 2005, "Film Cooling Performance in a Simulated Turbine Blade Tip Geometry," ASME Paper No. GT2005-68863.

[7] Ahn, J., Mhetras, S., and Han, J., 2005, "Film Cooling Effectiveness on a Gas Turbine Blade Tip Using Pressure Sensitive Paint," ASME Journal of Heat Transfer, Vol. 127, pp. 521-530.

[8] Hofer, T., and Arts, T., 2009, "Aerodynamic Investigation of the Tip Leakage Flow for Blades with Different Tip Squealer Geometries at Transonic Conditions," ASME Paper No. GT2009-59909.

[9] Zhou, C., Hodson, H., Tibbott, I., and Stokes, M., 2013, "The Aerothermal Performance of a Cooled Winglet Tip in a High Pressure Turbine Cascade," ASME J. Turbomach., 135, p. 031005.

[10] Narzary, D. P., Liu, K. C., Rallabandi, A. P., and Han, J. C., 2011, "Influence of Coolant Density on Turbine Blade Film-Cooling Using Pressure Sensitive Paint Technique," ASME J. Turbomach., 134, p. 031006.

[11] Li, S. J., Yang, S. F., and Han, J. C., 2013, "Effect of Coolant Density on Leading Edge Showerhead Film Cooling Using the Pressure Sensitive Paint Measurement Technique," ASME J. Turbomach., 136, p. 051011.

[12] Lu, K., Schobeiri, M. T., and Han, J. C., 2013, "Numerical Simulation of Film Cooling of Rotating Blade Tips within a High-Pressure Turbine," ASME Paper No. GT2013-94806.
[13] Mhetras, S., Narzary, D., Gao, Z., and Han, J. C., 2008, "Effect of a cutback squealer and cavity depth on film-cooling effectiveness on a gas turbine blade tip," ASME J. Turbomach., 130, p. 021002.
[14] Kwak, J. S., and Han, J. C., 2003, "Heat transfer coefficients and Film Cooling Effectiveness on the Squealer Tip of a Gas Turbine Blade," ASME J. Turbomach., Vol. 125, pp. 648-656.
[15] Chen, G., Dawes, W. N., and Hodson, H. P., 1993, "A Numerical and Experimental Investigation of Turbine Tip Gap Flow," 29th Joint Propulsion Conference and Exhibit, AIAA Paper No. 93-2253.
[16] Hohlfeld E. M., Christophel J. R., Couch E. L., and Thole K. A., 2005, "Predictions of Cooling From Dirt Purge Holes along the Tip of a Turbine Blade," International Journal of Turbo & Jet-Engines 22.3 (2005): 139-152.(ASME Paper No. GT2003-38251).
[17] Couch, E., Christophel, J., Hohlfeld, E., Thole, K. A., and Cunha, F. J., 2005, "Comparison of Measurements and Predictions for Blowing from the Tip of a Turbine Blade," AIAA Journal of Propulsion and Power, Vol. 21, No. 2, pp. 335-343.
[18] Krishnababu, S. K., Hodson, H. P., Booth, G. D., Lock, G. D., and Dawes, W. N., 2010, "Aerothermal Investigation of Tip Leakage Flow in a Film Cooled Industrial Turbine Rotor," ASME J. Turbomach., 132(2), pp. 1–9.
[19] Niu, M., and Zang, S., 2009, "Numerical Investigation of Active Tip-clearance Control through Tip Cooling Injection in an Axial Turbine Cascade," Journal of Thermal Science, Vol.18, No.4 pp. 306- 312(2009).
[20] Lim, C. H., Pullan, G., and Ireland, P., 2013, "Influence of Film Cooling Hole Angles and Geometries on Aerodynamic Loss and Net Heat Flux Reduction," ASME J. Turbomach., 135, p. 051019.
[21] Curtis, M. E., Denton, D. J., Longley, P. J., and Budimir, R., 2009, "Controlling Tip Leakage Flow Over a Shrouded Turbine Rotor Using an Air-Curtain," ASME Paper No. GT2009-59411.
[22] Hamik, M., and Willinger, R., 2007, "An Innovative Passive Tip-Leakage Control Method for Axial Turbines: Basic Concept and Performance Potential," ASME Journal of Thermal Science, Vol. 16, pp. 215-222.
[23] O'Dowd, D. O., Zhang, Q., He, L., Cheong, B. C. Y., and Tibbott, I., 2013, "Aero-thermal Performance of a Cooled Winglet at Engine Representative Mach and Reynolds Numbers, " ASME J. Turbomach., 135, p. 011041.
[24] Zhou, C., and Hodson, H., 2011, "The Tip Leakage Flow of an Unshrouded High Pressure Turbine Blade With Tip Cooling," ASME J. Turbomach., 133, p. 041028.
[25] Wheeler A.P.S., and Saleh Z., 2013, "Effect of Cooling Injection on Transonic Tip Flows," AIAA Journal of Propulsion and Power, DOI: 10.2514/1.B34657.
[26] Wheeler, A. P. S., Atkins, N. R., and He, L., 2011, "Turbine Blade Tip Heat Transfer in Low Speed and High Speed Flows," ASME J. Turbomach., 133, p. 041025.
[27] Zhang, Q., O'Dowd, D., He, L., Wheeler, A. P. S., Ligrani, P. M., and Cheong, B. C. Y., 2011, "Over-Tip Shock Wave Structure and Its Impact on Turbine Blade Tip Heat Transfer," ASME J. Turbomach., 133, p. 041001.
[28] Zhang, Q., and He, L., 2011, "Over-Tip Choking and Its Implications on Turbine Blade Tip Aerodynamic Performance," AIAA J. Propul. Power, 27(5), pp.1008–1014.
[29] Li W., Jiang H., Zhang Q., and Lee S. W., 2013, "Squealer tip leakage flow Characteristics in transonic condition," in press with ASME Journal of Engineering for Gas Turbines and Power. (ASME GT 2013-95283).
[30] Felix J. W., 1963, "Optics of Flames-Including Methods for the Study of Refractive Index Fields in Combustion ans Aerodynamics," Butterworths, London, 1963. DIO: 10.1002/ange. 19640760623
[31] Wolfgang M., 1987, "Flow Visualization," Academic Press, Inc., 1987. ISBN 0-12-491351-2.
[32] Lakshminarayana B., 1996, "Fluid Dynamics and Heat Transfer of Turbomachinery," John Wiley & Sons, Inc., 1996. ISBN 0-471-85546-4.